DOI: 10.1002/ejic.200501111

Relationship Between the Nearest-Neighbor Exchange Coupling Constants and the Number of Exchange Interactions in the Cyano-Bridged $MnMo_6(CN)_{18}$ Cluster: Density Functional Theory Calculations

Yi-Quan Zhang*[a] and Cheng-Lin Luo[a]

Keywords: Molecular magnetism / Density functional calculations / Broken symmetry / Cyano-bridged clusters / Single-molecule studies

A theoretical density functional study of the relationship between the nearest-neighbor MnMo constants and the number of exchange interactions in the cyano-bridged $K[(Me_3tacn)_6MnMo_6(CN)_{18}](ClO_4)_3$ cluster is presented. Two approaches (the first approach consisted of evaluating the exchange coupling constant J_{ij} between two paramagnetic metal centers *i* and *j* in the hexanuclear molecule by calculating the energy differences between the highest and broken-symmetry spin states of a model molecule in which metal atoms except for *i* and *j* are substituted by diamagnetic Y^{III} cations, and the second is to calculate the different spin-state energies of hexanuclear complexes and use the Heisenberg Hamiltonian to obtain the exchange coupling constants between different metal centers) show that the antiferromagnetic coupling interactions between nearest neighbors weaken with the increase of the number of exchange interactions. The various θ angles have an influence on the interactions between the nearest-neighbor MoMn but do not change the trend between J_{12} and the number of exchange interactions. Moreover, Kahn's qualitative theory succeeded in being applied to interpret the trend.

Introduction

In recent years, the synthesis and study of single-molecule magnets with high total spin that can be used to store potential data have received much attention.[1–14] In these single-molecule magnets, much attention is focused on developing cyano-bridged cluster systems, for which the parameters S and D are more readily adjusted by substitution of various metal ions.[5–14] Long and coworkers found that the absolute nearest-neighbor constants *J* always diminish as the number of exchange interactions increases for a series of cyano-bridged Mn^{II}–Cr^{III},[5,6] Mn^{III}–Cr^{III},[7–9] Mo^{III}–Ni^{II},[10] and Cr^{III}–Ni^{II} [11,12] complexes. It was demonstrated that the interactions between the nearest-neighbor Mn^{III} and Cr^{III} decrease with the increase of the number of exchange interactions when we investigated the magnetism of the cyano-bridged $\{Cr[CNMn(salen)(H_2O)]_6\}^{3+}$ [7,8] cluster and the linear trinuclear $[(5\text{-}Brsalen)_2(H_2O)_2Mn_2Cr(CN)_6]$[9] cluster.[13] For the cyano-bridged single-molecule cluster $K[(Me_3tacn)_6MnMo_6(CN)_{18}](ClO_4)_3$,[14] which has a substantial increase in the nearest-neighbor MnMo interactions compared to those of the above MnCr complexes, we want to know whether the above trend also exists. and whether the MoMnMo angle has an influence on the interactions between the nearest neighbors. Kahn's qualitative theory[15,16] was used to interpret the relationship. Finally, we will discuss the relationship between the calculated spin-density populations on Mn^{II} or Mo^{III} and the number of exchange interactions.

Computational Methodology

Description of the Complexes and Models

In calculations, we used model $\mathbf{A^6}$ $[(Me_3tacn)_6Mn\text{-}Mo_6(CN)_{18}]^{2+}$, which is a polynuclear cluster in which six $[(Me_3tacn)Mo(CN)_3]$ units surround a central Mn^{II} ion (see Figure 1) and was directly taken from complex $K[(Me_3tacn)_6MnMo_6(CN)_{18}](ClO_4)_3$[14] and not optimized. The bridges are of the Mo–CN–Mn type and, therefore, the Mn atom with an N_6 coordination sphere is in a high-spin configuration. Models $\mathbf{A^1}$, $\mathbf{A^2}$, $\mathbf{A^3}$, $\mathbf{A^4}$, and $\mathbf{A^5}$ (the superscript numbers denote the number of exchange interactions) (see Figure 2) were used to investigate the relationship between the nearest-neighbor exchange coupling constants J_{12} and the number of exchange interactions. To investigate the relationship between J_{12} and the θ angle (we use θ to represent the MoMnMo angle), we obtained three different structures that all include two of the exchange interactions $\mathbf{A^2}$, $\mathbf{A^{2\prime}}$, and $\mathbf{A^{2\prime\prime}}$ (see Figure 3). The θ angles for $\mathbf{A^2}$, $\mathbf{A^{2\prime}}$, and $\mathbf{A^{2\prime\prime}}$ are 86.38°, 113.33°, and 154.92°, respectively. All the mod-

---

[a] School of Physical Science and Technology, Nanjing Normal University,
Nanjing 210097, China
E-mail: zhangyiquan@pine.njnu.edu.cn

els were directly taken from model **A⁶**, and not optimized because small changes to the experimental structures could result in significant deviations for the coupling constants. To easily perceive the topology of the metal framework, we used sticks for the carbons of the tacn ligands and the terminal CN ligands in Figure 1, Figure 2, and Figure 3.

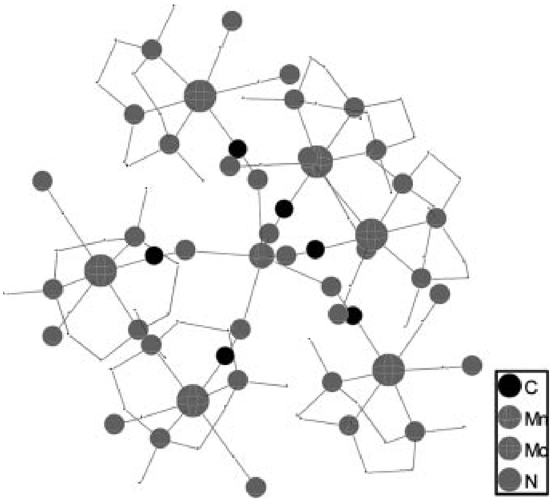

Figure 1. Structure of model **A^6** ($MnMo_6$).

Calculation on Exchange Coupling Constant

There are two different approaches to calculating the exchange coupling constants for the polynuclear complexes.[17–19] In all calculations, the spin-orbit coupling is not considered, so the magnetic anisotropy does not need to be considered. The first approach consisted of evaluating the exchange coupling constant J_{ij} between two paramagnetic metal centers i and j in the hexanuclear molecule by calculating the energy difference between the highest and broken-symmetry spin states of a model molecule in which metal atoms except for i and j are substituted by diamagnetic Y^{III} cations. This approach was used to calculate the exchange coupling interactions of hexanuclear complexes in many papers and proved to give good results compared to the experimental ones.[17–20] The second approach is to calculate the different spin-state energies of hexanuclear complexes and use the Heisenberg Hamiltonian to obtain the exchange coupling constants between different metal centers.[17–21] It is a more rigorous approach in evaluating J for polynuclear complexes than the first one. How to use these two approaches will be interpreted thoroughly below.

For the first approach, the magnetic interactions between Mn^{II} and Mo^{III} metal ions were studied on the basis of density functional theory (DFT) coupled with the broken-symmetry approach (BS).[22–24] The exchange coupling constants J were evaluated by calculating the energy difference

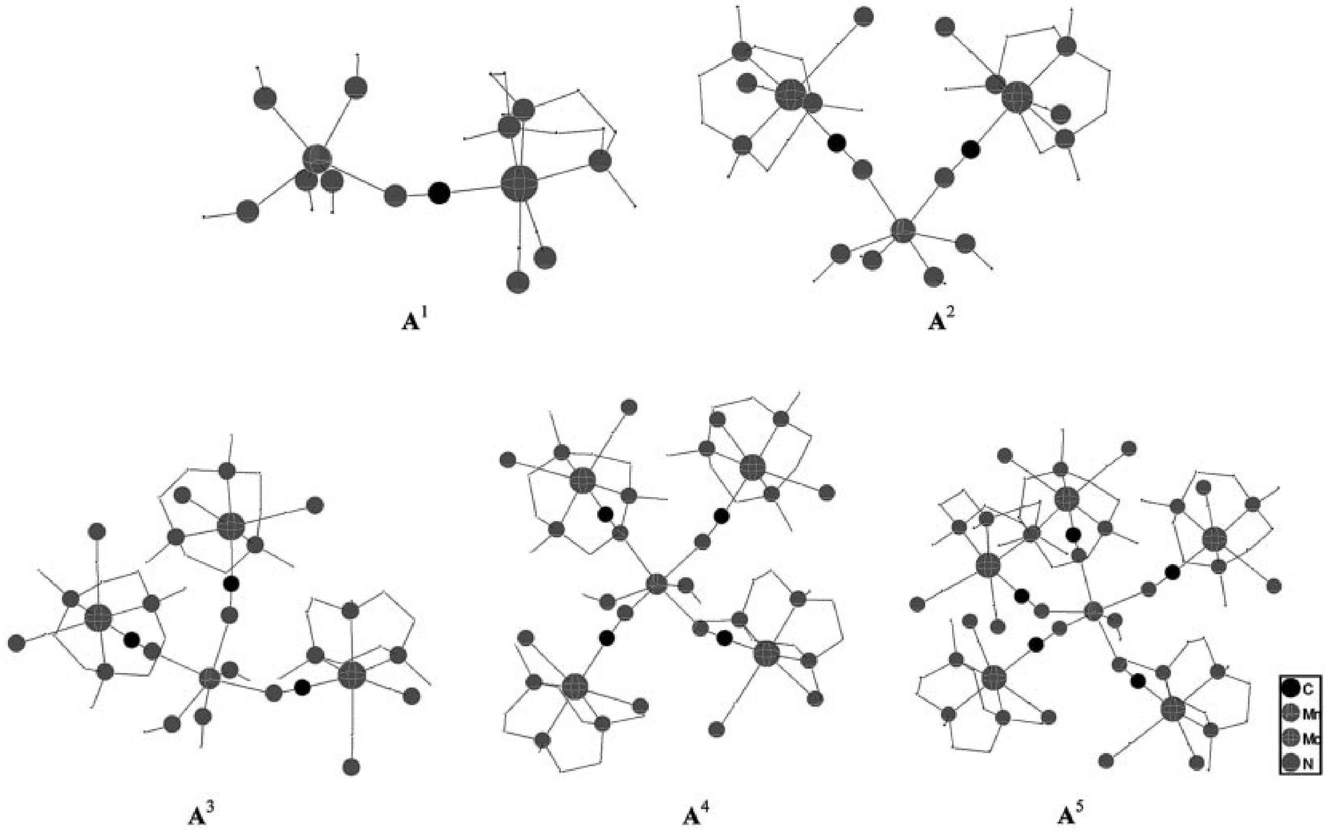

Figure 2. Structure of models **A^1** (MnMo), **A^2** ($MnMo_2$), **A^3** ($MnMo_3$), **A^4** ($MnMo_4$), and **A^5** ($MnMo_5$).

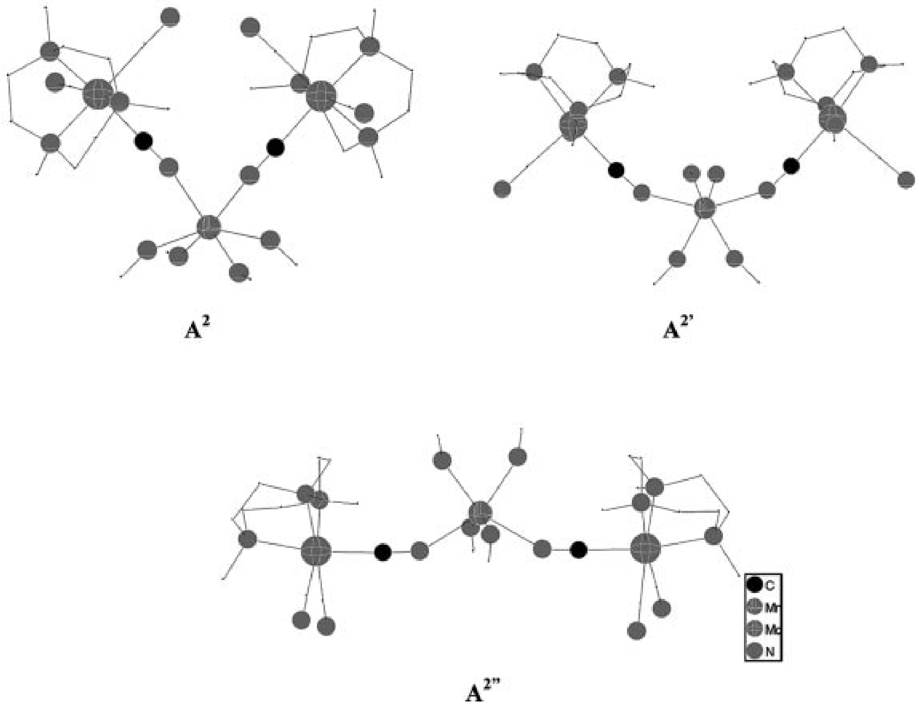

Figure 3. Structure of models $\mathbf{A^2}$ (θ = 86.38°), $\mathbf{A^{2'}}$ (θ = 113.33°), and $\mathbf{A^{2''}}$ (θ = 154.92°).

between the high-spin state (E_{HS}) and the broken-symmetry state (E_{BS}). Assume the spin Hamiltonian is defined as Equation (1).

$$\hat{H} = -2J\hat{S}_1\cdot\hat{S}_2 \tag{1}$$

If the spin-projected approach is used, the equation proposed by Noodleman[22–24] to extract the J value for a binuclear transition-metal complex is thus Equation (2).

$$J = \frac{E_{BS} - E_{HS}}{4S_1S_2} \tag{2}$$

while with the nonprojected approach:[25]

$$2J = \frac{E_{BS} - E_{HS}}{2S_1S_2 + S_2} \tag{3}$$

where S_1 and S_2 are the total spins of two interacting paramagnetic centers and $S_1 > S_2$ is assumed for heterodinuclear complexes.

However, Equation (3) corresponds strictly to the limit of complete overlap between the magnetic orbitals and such a hypothesis is not sustained,[26] although it can give good J results compared to the experimental ones.[25,27,28]

For all models, where S_1 = 5/2 for $\mathrm{Mn^{II}}$ and S_2 = 3/2 for $\mathrm{Mo^{III}}$, from Equation (2) we get Equation (4).

$$J = (E_{BS} - E_{HS})/15 \tag{4}$$

The second approach is more rigorous. If one neglects the spin-orbit coupling effects, the Hamiltonian for a general extended structure is indicated in Equation (5).

$$\hat{H} = \sum_{i>j} -2J_{ij}\hat{S}_i\hat{S}_j \tag{5}$$

where $\hat{S}_i$ and $\hat{S}_j$ are the spin operators of the different paramagnetic centers. The J_{ij} values are the coupling constants between all the paramagnetic centers. In our paper, we only consider the exchange interactions between nearest neighbors. This fact together with the presence of additional symmetry elements in the structure normally result in a reduced set of J_{ij} values.

When using single-determinant methods such as DFT, the calculated energies are related to the diagonal matrix elements of the Heisenberg Hamiltonian. An alternative way to describe the system is by considering an Ising Hamiltonian as a special case of a Heisenberg Hamiltonian in which only the diagonal terms are kept. Thus, we can consider that the wave functions obtained with the single-determinant methods are eigenfunctions of an Ising Hamiltonian that is formulated with the same J values as the original Heisenberg Hamiltonian because their diagonal terms are identical. For that reason, the J values obtained with single-determinant methods are directly comparable to those obtained from experimental data.[19] So we can use the single-dominant method DFT to obtain the J values from calculating the energy differences between two spin-states. A thorough description of this approach can be found in refs.[17–19,21]

For $\mathbf{A^2}$, which includes three magnetic centers, the magnetic coupling constants J_{12} between each nearest-neighbor $\mathrm{Mo^{III}}$–$\mathrm{Mn^{II}}$ pair are the same for the symmetry of the complete structure. Moreover, we only need the nearest-neighbor coupling constant. So, the J_{12} can be extracted by calculating the energies of two spin-states: **1** with $S = 1/2$, and **2** with $S = 11/2$, which are shown in Figure 4. The equation to extract J_{12} is thus Equation (6).

$$J_{12} = (E_1 - E_2)/35 \tag{6}$$

Figure 4. Two spin states: **1** with $S = 1/2$ (left), **2** with $S = 11/2$ (right) for model $\mathbf{A^2}$.

To obtain all the nearest-neighbor constants J_{12} for the modeled structures $\mathbf{A^3}$, $\mathbf{A^4}$, $\mathbf{A^5}$, and $\mathbf{A^6}$, we also only need to calculate the energy of two spin-states for each model. Two spin-states for each model are as follows: **1** with $S = 1/2$ and **2** with $S = 11/2$ for $\mathbf{A^2}$, **1** with $S = 2$ and **2** with $S = 14/2$ for $\mathbf{A^3}$, **1** with $S = 7/2$ and **2** with $S = 17/2$ for $\mathbf{A^4}$, **1** with $S = 5$ and **2** with $S = 10$ for $\mathbf{A^5}$, and **1** with $S = 13/2$ and **2** with $S = 23/2$ for $\mathbf{A^6}$. For all these **1** states, only the spins on $\mathrm{Mn^{II}}$ are flipped. The equations to extract J_{12} values for all of the models are as follows:
For model $\mathbf{A^3}$, Equation (7) is thus:

$$J_{12} = (E_1 - E_2)/50 \tag{7}$$

For model $\mathbf{A^4}$, Equation (8) is thus:

$$J_{12} = (E_1 - E_2)/65 \tag{8}$$

For model $\mathbf{A^5}$, Equation (9) is thus:

$$J_{12} = (E_1 - E_2)/80 \tag{9}$$

For model $\mathbf{A^6}$, Equation (10) is thus:

$$J_{12} = (E_1 - E_2)/95 \tag{10}$$

DFT calculations have been performed using the Amsterdam Density Functional (ADF, version 2004.01[29–31]) package for four models. Illas et al.[32] showed the strong dependence of the calculated J with respect to the exchange-correlation functionals chosen. Several exchange-correlation functionals will be used to evaluate J. In the calculations of J using ADF, the local density approximation (LDA) made use of the Vosko, Wilk, and Nusair[33] (VWN) local correlation functional. A series of generalized gradient approximation (GGA): Perdew-Wang 1991 (PW91),[34] Perdew-Burke-Ernzerhof (PBE),[35] and the recently developed OPTX-Perdew (Operdew)[36,37] and OPTX-Perdew–Burke–Ernzerhof (OPBE)[35–37] functionals were examined. Basis set TZV2P [a basis set of triple-ζ quality[38] supplemented with two p orbitals ("polarization functions")] was applied for all of the metals (Mo, Mn) and basis set DZP (a basis set of double-ζ quality[38] supplemented with one polarization function) for the other atoms (C, N, and H). The inner core shells of C(1s), N(1s), Mn(1s, 2s, 2p), Y(1s, 2s, 2p, 3s, 3p), and Mo(1s, 2s, 2p, 3s, 3p) were treated by the frozen core approximation. The accuracy parameter (accint) for the numerical integration grid was set to 4.0 for all of the complexes. The convergence standard of the system energy was set to be smaller than 10^{-6} eV, reaching a precision required for the evaluation of J.

Results and Discussion

Relationship Between *J* and the Number of Exchange Interactions

The relationship between the nearest-neighbor exchange coupling constants J_{12} and the number of exchange interactions is shown in Figure 5. Two approaches show that the absolute J_{12} values decrease with the increase of the number of exchange interactions. The second approach gives better results than the first one for $\mathbf{A^2}$, $\mathbf{A^{2\prime}}$, and $\mathbf{A^{2\prime\prime}}$. However, the two approaches give similar results for $\mathbf{A^3}$, $\mathbf{A^4}$, $\mathbf{A^5}$, and $\mathbf{A^6}$. This is because the decrease of the absolute J_{12} values with the increase of the number of exchange interactions will reduce the differences between the results using the two approaches. Moreover, this is of conceptual importance, as the

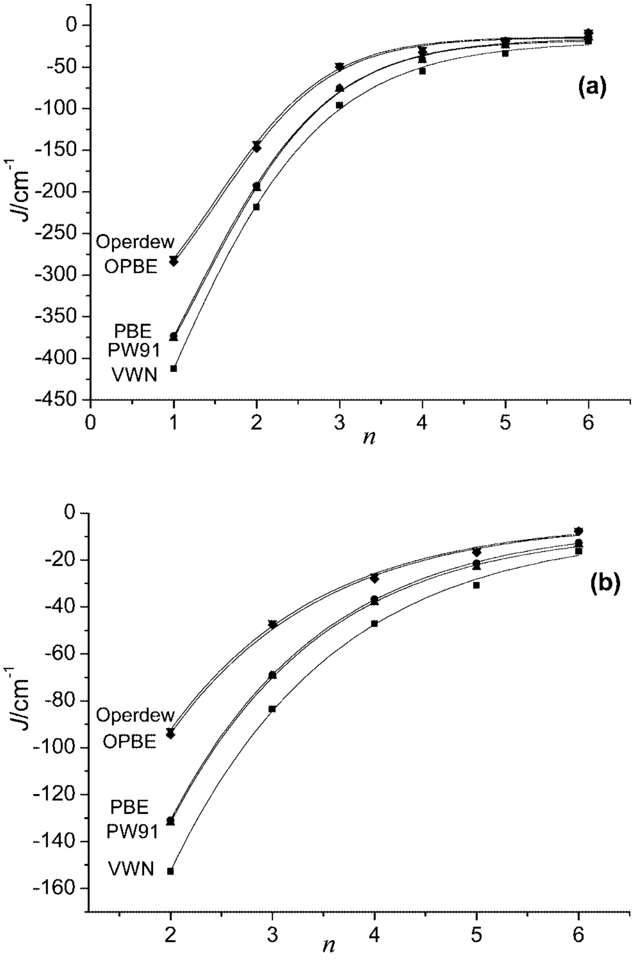

Figure 5. Relationship between the nearest-neighbor interaction constant J_{12} (cm^{-1}) and the number of exchange interactions n with several functionals [VWN (■), PW91 (●), PBE (▲), Operdew (▼), and OPBE (♦)] for the models of complex **I**. (a) The relationship using the first approach; (b) the relationship using the second approach.

Table 1. Experimental J_{12} value for the complete structure and calculated J_{12} values (cm^{-1}) for models $\mathbf{A^1}$, $\mathbf{A^2}$, $\mathbf{A^{2'}}$, $\mathbf{A^{2''}}$, $\mathbf{A^3}$, and $\mathbf{A^6}$ using two approaches with different functionals in ADF.

	Approach	VWN	PW91	PBE	Operdew	OPBE	Experiment
$\mathbf{A^1}$	first	–412.3	–373.2	–375.7	–280.1	–284.2	–6.7[10]
$\mathbf{A^2}$	first	–218.0	–192.5	–195.8	–142.0	–147.2	
	second	–152.7	–130.9	–132.0	–92.7	–94.4	
$\mathbf{A^{2'}}$	first	–208.2	–183.2	–184.8	–133.0	–136.3	
	second	–147.9	–127.3	–128.3	–89.4	–91.4	
$\mathbf{A^{2''}}$	first	–164.4	–132.8	–133.9	–84.6	–87.7	
	second	–123.1	–98.4	–99.2	–62.4	–64.4	
$\mathbf{A^3}$	first	–95.8	–75.4	–76.1	–48.1	–50.1	
	second	–83.6	–68.9	–69.5	–46.7	–47.7	
$\mathbf{A^6}$	first	–18.7	–13.4	–14.8	–8.6	–9.0	
	second	–16.3	–12.6	–13.5	–7.4	–7.7	

changes in J_{12} values with the number of Mo atoms has to do with the fact that one new t_{2g} orbital is incorporated in the exchange interaction for the first three Mo atoms, then the addition of new atoms does not introduce new orbital interactions, as reflected in the small slopes between $n = 3$ and $n = 6$. From Figure 5, the consistent behavior between the calculated J_{12} values and the experimental value becomes better in the sequence: LDA (VWN), GGA (PW91, PBE), GGA (Operdew, OPBE), which was also found in our previous paper,[13] and the differences between the calculated J_{12} values using the two approaches decrease with the increase of the number of exchange interactions for all of the functionals. From Table 1, the calculated J_{12} values of model $\mathbf{A^6}$, which is the most similar to the complete structure using two approaches with Operdew and OPBE functionals, have good agreement with the experimental result.[14]

The nearest-neighbor exchange coupling constants J_{12} calculated using different functionals with two approaches for models $\mathbf{A^2}$, $\mathbf{A^{2'}}$, and $\mathbf{A^{2''}}$ are shown in Table 1 where the absolute J_{12} values calculated using two approaches with all the functionals all decrease with the increase of the θ angle. From Table 1, we also found that the increase of the J_{12} values from $\mathbf{A^2}$ to $\mathbf{A^{2'}}$ is very small but large from $\mathbf{A^{2'}}$ to $\mathbf{A^{2''}}$. However, all the J_{12} values of models $\mathbf{A^2}$, $\mathbf{A^{2'}}$, and $\mathbf{A^{2''}}$ are between those of $\mathbf{A^1}$ and $\mathbf{A^3}$ and thus, the different θ angles do not change the trend between J_{12} and the number of exchange interactions.

Qualitative Analysis of the Exchange Interaction

According to Kahn's theory,[15,16] the exchange coupling constant J is expressed in Equation (11) ($\hat{H} = -2J\hat{S}_1 \cdot \hat{S}_2$).

$$J_{ab} \approx K_{ab} - S_{ab}(\Delta^2 - \delta^2)^{1/2} \qquad (11)$$

The positive term K_{ab} represents the ferromagnetic contribution J_F, favoring parallel alignment of the spins and a triplet ground state, while the negative term $-S_{ab}(\Delta^2 - \delta^2)^{1/2}$ is the antiferromagnetic contribution J_{AF}, favoring antiparallel alignment of the spins and a singlet ground state. S_{ab} is the overlap integrals between **a** and **b**. δ is the initial energy gap between the magnetic orbitals, and Δ the energy gap between the molecular orbitals derived from them. When several electrons are present on each center, n_A on one side, n_B on the other, J can be described by the sum of the different "orbital pathways" J_{ab}, defined as above for pairs of orbitals **a** and **b** located on each site, weighted by the number of electrons [Equation (12)].

$$J = \sum_{a,b} J_{ab}/n_A n_B \qquad (12)$$

Some authors[39,40] have recently shown that magnetic orbitals **a** and **b** are well represented by the localized orbitals of the broken-symmetry solution (they call them BS-OMSO[41]). There are 15 different contributions to the exchange coupling constant in each $\mathrm{Mo^{III}}$–$\mathrm{Mn^{II}}$ pair; the inappropriate orientation of some of the magnetic orbitals involved allows us to discard most of them. The ferromagnetic contributions are not considered because the antiferromagnetic coupling interactions for all the complexes are dominant. Moreover, as usual, the changes in the J_{AF} term are more important and these contributions usually control the magnetostructural correlations, especially for those whose intramolecular interactions are antiferromagnetic. Hence, we only consider the changes in the J_{AF} term. Among the important antiferromagnetic contributions, the most relevant ones are those involving two t_{2g} orbitals (d_{xy} and d_{xz}) of the $\mathrm{Mo^{III,}}$ which are directed toward the bridging ligands because of the good overlap with the appropriate t_{2g} orbitals (d_{xy} and d_{xz}) of the $\mathrm{Mn^{II}}$. The mean overlap integral S_{ij} between the four orbitals of the $\mathrm{Mo^{III}}$ and $\mathrm{Mn^{II}}$ can be expressed as Equation (13).

$$S_{ij} = 1/4(d_{xy}d_{xy} + d_{xy}d_{xz} + d_{xz}d_{xy} + d_{xz}d_{xz}) \qquad (13)$$

Figure 6 gives the relationship between J_{12} and S_{ij} obtained using Equation (13) and the PW91 functional with the increase of the number of the exchange interaction. The absolute J_{12} values decrease with the decrease of the S_{ij} in accordance with Kahn's qualitative theory. Therefore, we can conclude that the increase of the number of exchange interactions will decrease the overlap integral S_{ij} and lead to the decrease of the absolute J_{12} values. This conclusion can be verified by investigating the relationship between J_{12} and the spin-density populations on $\mathrm{Mo^{III}}$ and $\mathrm{Mn^{II}}$ with the increase of the number of exchange interactions. Because the spin-density populations on several $\mathrm{Mo^{II}}$ are al-most the same, we only use the spin-density population on one Mo^{II}. The spin-density populations on Mo^{III} and Mn^{II} were obtained with Mulliken Population Analysis[42] calculated using the PW91 functional in the ADF2004.01 package in the high-spin (HS) states. The relationship is shown in Figure 7 where the spin populations on Mo^{III} and Mn^{II} increase with the decrease of the absolute J_{12}. From Kahn's theory, the increase of the spin populations on Mo^{III} and Mn^{II} will decrease the S_{ij} and then lead to the decrease of the absolute J_{12}. Moreover, we also found that the various spin populations on Mn^{II} were much smaller than those on Mo^{III}. These results were calculated using the first approach. The second approach also gives the same trend between J_{12} and the spin-density populations on Mo^{III} and Mn^{II} in the high-spin states.

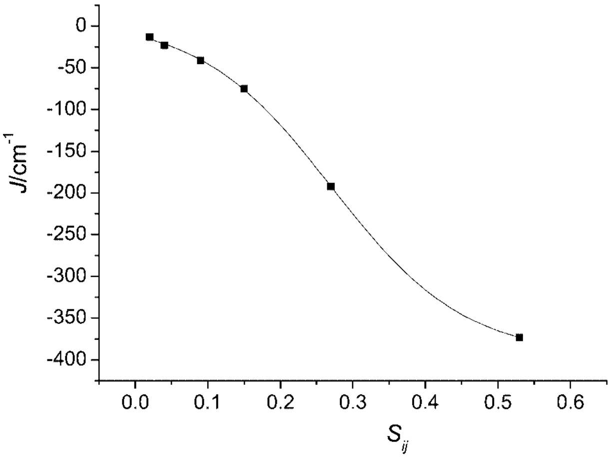

Figure 6. Relationship between the nearest-neighbor interaction constant J_{12} (cm^{-1}) and the mean overlap integral S_{ij} with the increase of the number of exchange interactions using the PW91 functional.

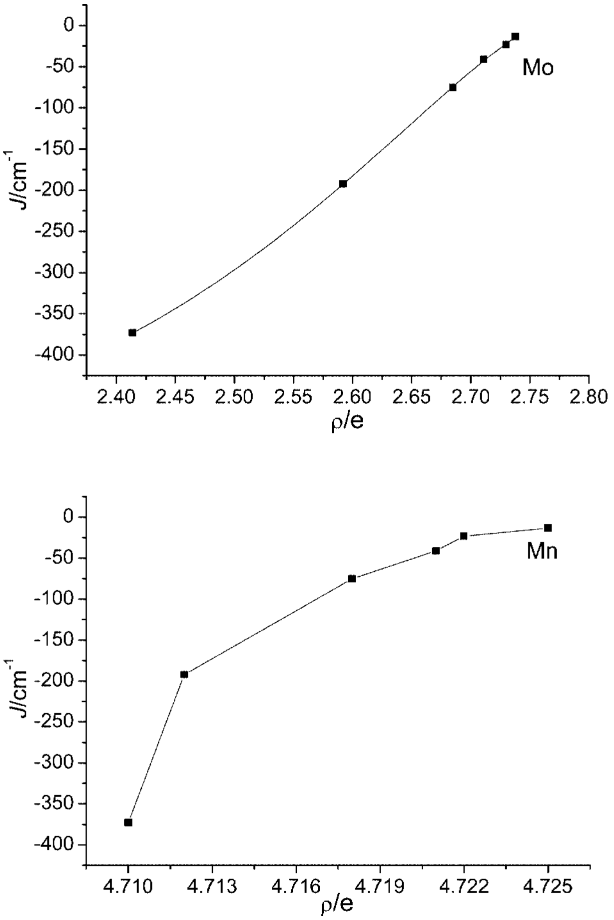

Figure 7. Relationship between the nearest-neighbor interaction constant J_{12} (cm^{-1}) and the spin-density populations ρ on Mo^{III} (top) and Mn^{II} (bottom) in the high-spin states with the PW91 functional using the first approach.

Conclusions

Two approaches were used to investigate the magnetic coupling interactions between the nearest-neighbor Mo^{III} and Mn^{II}. From our calculations, both approaches show that the antiferromagnetic interactions between nearest-neighbors decrease with the increase of the number of exchange interactions for our studied Mo^{III}–Mn^{II} system. The trend is rationalized by using Kahn's theory through the overlap integral S_{ij} and the spin-density populations on Mo^{III} and Mn^{II} in the HS states successfully. The absolute J_{12} values calculated using two approaches with all the functionals all decrease with the increase of the θ angle, and the decrease of the absolute J_{12} values from $\mathbf{A^2}$ to $\mathbf{A^{2'}}$ is very small but large from $\mathbf{A^{2'}}$ to $\mathbf{A^{2''}}$. However, all the J_{12} values of models $\mathbf{A^2}$, $\mathbf{A^{2'}}$, and $\mathbf{A^{2''}}$ are between those of $\mathbf{A^1}$ and $\mathbf{A^3}$ and, thus, the different θ angles do not change the trend between J_{12} and the number of exchange interactions.

Acknowledgments

This project is supported by the Natural Science Foundation of Jiangsu Province of China, the Natural Science Foundation of University of Jiangsu Province of China (Grant No. 05KJB150055), and the Natural Science Foundation of Nanjing Normal University of China (Grant No. 111080B142).

---

[1] O. Kahn, C. J. Martinez, *Science* **1998**, *279*, 44–48.
[2] R. Sessoli, D. Gatteschi, A. Caneschi, M. A. Novak, *Nature* **1993**, *365*, 141–143.
[3] Y. Q. Zhang, C. L. Luo, Z. Yu, *New J. Chem.* **2005**, *29*, 1285–1290.
[4] Y. Q. Zhang, C. L. Luo, Z. Yu, *Int. J. Quantum Chem.* **2005**, *102*, 165–173.
[5] J. L. Heinrich, J. J. Sokol, A. G. Hee, J. R. Long, *J. Solid State Chem.* **2001**, *159*, 293–301.
[6] L. Toma, R. Lescouezec, J. Vaissermann, F. S. Delgado, C. Ruiz-Perez, R. Carrasco, J. Cano, F. Lloret, M. Julve, *Chem. Eur. J.* **2004**, *10*, 6130–6145.
[7] H. J. Choi, J. J. Sokol, J. R. Long, *J. Phys. Chem. Solids* **2004**, *65*, 839–844.
[8] X. Shen, B. Li, J. Zou, Z. Xu, *Transition Met. Chem.* **2002**, *27*, 372–376.
[9] H. J. Choi, J. J. Sokol, J. R. Long, *Inorg. Chem.* **2004**, *43*, 1606–1608.
[10] M. P. Shores, J. J. Sokol, J. R. Long, *J. Am. Chem. Soc.* **2002**, *124*, 2279–2292.
[11] P. A. Berseth, J. J. Sokol, M. P. Shores, J. L. Heinrich, J. R. Long, *J. Am. Chem. Soc.* **2000**, *122*, 9655–9662.

[12] T. Mallah, C. Auberger, M. Verdaguer, P. J. Veillet, *Chem. Soc., Chem. Commun.* **1995**, 61–62.
[13] Y. Q. Zhang, C. L. Luo, *J. Phys. Chem. A*, in press.
[14] J. J. Sokol, A. G. Hee, J. R. Long, *J. Am. Chem. Soc.* **2002**, *124*, 7656–7657.
[15] O. Kahn, B. J. Briat, *Chem. Soc. Faraday Trans.* **1976**, *72*, 268–281.
[16] J. J. Girerd, Y. Journaux, O. Kahn, *Chem. Phys. Lett.* **1981**, *82*, 534–538.
[17] E. Ruiz, J. Cano, S. Alvarez, A. Caneschi, D. Gatteschi, *J. Am. Chem. Soc.* **2003**, *125*, 6791–6794.
[18] E. Ruiz, A. Rodríguez-Fortea, P. Alemany, S. Alvarez, *Polyhedron* **2001**, *20*, 1323–1327.
[19] E. Ruiz, M. Llunell, P. Alemany, *J. Solid State Chem.* **2003**, *176*, 400–411.
[20] E. Ruiz, A. Rodríguez-Fortea, J. Cano, S. Alvarez, P. Alemany, *J. Comput. Chem.* **2003**, *24*, 982–989.
[21] O. Kahn, *Molecular Magnetism*, VCH Publishers, New York, **1993**, pp. 211–236.
[22] L. Noodleman, *J. Chem. Phys.* **1981**, *74*, 5737–5743.
[23] L. Noodleman, E. J. Baerends, *J. Am. Chem. Soc.* **1984**, *106*, 2316–2327.
[24] L. Noodleman, D. A. Case, *Adv. Inorg. Chem.* **1992**, *38*, 423–432.
[25] E. Ruiz, J. Cano, S. Awarez, P. Alemany, *J. Comput. Chem.* **1999**, *20*, 1391–1400.
[26] R. Caballol, O. Castell, F. Illas, I. de P. R. Moreira, J. P. Malrieu, *J. Phys. Chem. A* **1997**, *101*, 7860–7866.
[27] E. Ruiz, P. Alemany, S. Alvarez, J. Cano, *Inorg. Chem.* **1997**, *36*, 3683–3688.
[28] A. Rodríguez-Fortea, P. Alemany, S. Alvarez, E. Ruiz, *Chem. Eur. J.* **2001**, *7*, 627–637.
[29] F. M. te Velde, G. Bickelhaupt, S. J. A. van Gisbergen, C. Fonseca Guerra, E. J. Baerends, J. G. Snijders, T. Ziegler, *J. Comput. Chem.* **2001**, *22*, 931–967.
[30] C. Fonseca Guerra, G. J. G. Snijders, F. M. te Velde, E. J. Baerends, *Theor. Chem. Acc.* **1998**, *99*, 391–403.
[31] ADF2004.01, SCM, Theoretical Chemistry, Vrije Universiteit, Amsterdam, The Netherlands, http://www.scm.com.
[32] F. Illas, I. de P. R. Moreira, J. M. Bofill, M. Filatov, *Phys. Rev. B* **2004**, *70*, 132414.
[33] S. H. Vosko, L. Wilk, M. Nusair, *Can. J. Phys.* **1980**, *58*, 1200.
[34] J. P. Perdew, J. A. Chevary, S. H. Vosko, K. A. Jackson, M. R. Pederson, D. J. Singh, C. Fiolhais, *Phys. Rev. B* **1992**, *46*, 6671–6687.
[35] J. P. Perdew, K. Burke, M. Ernzerhof, *Phys. Rev. Lett.* **1996**, *77*, 3865–3868.
[36] N. C. Handy, A. J. Cohen, *Mol. Phys.* **2001**, *99*, 403–412.
[37] J. P. Perdew, *Phys. Rev. B* **1986**, *33*, 8822–8824.
[38] A. Schaefer, C. Huber, R. Ahlrichs, *J. Chem. Phys.* **1994**, *100*, 5829–5835.
[39] F. Fabrizi de Biani, E. Ruiz, J. Cano, J. J. Novoa, S. Alvarez, *Inorg. Chem.* **2000**, *39*, 3221–3229.
[40] C. Blanchet-Boiteux, J. M. Mouesca, *Theor. Chem. Acc.* **2000**, *104*, 257–264.
[41] C. Desplanches, E. Ruiz, A. Rodríguez-Fortea, *J. Am. Chem. Soc.* **2002**, *124*, 5197–5205.
[42] A. Szabo, N. S. Ostlund, *Modern Quantum Chemistry*, McGraw-Hill, New York, **1989**.

Received: December 13, 2005